Further Improvement of Super-Resolution Reconstruction

Edward Y. T. Ho*, Andrew E. Todd-Pokropek
Department of Medical Physics and Bioengineering, University College London
London WC1E 6BT, United Kingdom
*edwardho@medphys.ucl.ac.uk

***Abstract* — We propose a novel approach to improve further the quality of recovered images from standard super-resolution reconstruction, using Lewitt's Kaiser-Bessel window functions (blobs) as the basis functions instead of normal pixels or voxels. The spatially localised and rotationally symmetric properties of blobs have made them very attractive for iterative image reconstruction. However, these same properties of blobs can be also very advantageous for super-resolution recovery, when more than one of a similar 2D or 3D scene is available. We show in this paper that by incorporating blobs into the super-resolution algorithm for image recovery; we can obtain much better quality, especially when there are only a few lower quality images available for the same scene. Moreover, using fewer low-resolution images for super-resolution reconstruction, we can also guarantee improvement in computational time.**

***Index Terms* — Super-resolution, Kaiser-Bessel window functions (blobs)**

I. Introduction

Reconstruction algorithms are usually approximated by a linear combination of known basis functions and greatly influence the outcome of the reconstruction algorithms. The basis functions that are commonly used are those, having a unit value inside a cubic volume and zero outside, known as cubic voxels, for example in 3D. The resulting approximations from using cubic voxels have undesirable artificial sharp edges; therefore it appears to be more appropriate to use basis functions with a smooth transition from one to zero. Lewitt et. al. [1, 2, 3, 4] have proposed the use of the modified Kaiser-Bessel window functions, commonly known as blobs to be the basis functions for image reconstruction. The main characteristics of the blobs include :

- blobs are spatially localized
- blobs are rotationally symmetric
- their Fourier transform are effectively localized, i.e. they are almost band-limited
- there are analytical formulas for computing in n-dimensions of their projections, Fourier transforms, gradients and Laplacians
- blobs are constructed to have any finite number of continuous derivatives
- blobs act as low-pass filters, suppressing high-frequency noise

Super-resolution is the process of combining multiple low-resolution images of the same scene to produce an image of superior quality. Information contained within the low-resolution images has to be overlapped accurately in order to produce the super-resolution image. Early attempts of super-resolution framework were based on the generalised sampling theorem [5] and restoration in the frequency domain [6]. Other recent approaches include using projection onto convex sets to solve iteratively the super-resolution inverse model [7,8]. The above authors assumed that the scene intensities are a continuous function. However, in order to re-define the super-resolution reconstruction in an optimisation framework, a suitable discrete representation of the scene intensities is necessary for the super-resolution imaging model. Some related literatures on generative models include a simpler motion of pure translation [9], Euclidean transformation [10] and affine transformation [11]. In [12], Capel and Zisserman used a rectangular window PSF and in [13], Irani and Peleg used their well-known image registration approach for super-resolution reconstruction. Other approaches include reconstruction based on a sequence of images with different zoom factors [14]. Rajan and Chaudhuri [15,16] used generalised interpolation to interpolate decomposed image data on individual subspaces before transforming them back into the image domain. Literatures of other super-resolution framework can be found in [17].

In this paper, we use Capel's [18] generative imaging model for the super-resolution reconstruction. However, we use blobs as the basis functions in our iterative image reconstruction algorithm.

II. Theoretical Background

A. Modified Kaiser-Bessel Window Functions (Blobs)

In iterative image reconstruction techniques, we approximate a density function, $\overline{f}(x,y,z)$ representing the reconstructed image using a linear combination of a set of coefficients, $\{c_j\}$ and known basis functions, $\Phi(x-x_j, y-y_j, z-z_j)$, where $\{x_j, y_j, z_j\}$ is the usual orthogonal axes in the Cartesian coordinates.

$$\overline{f}(x,y,z) = \sum_{j=1}^{J} c_j \Phi(x-x_j, y-y_j, z-z_j) \qquad (1)$$

As suggested above, in this case we choose blobs, $b(r)=b\left(\sqrt{x^2+y^2+z^2}\right)$ to be our basis functions rather than the conventional voxel basis functions and we are able to define the density function using a single variable, i.e. the radial coordinate, r because of the spherically symmetric property of blobs. Blobs are functions of rotationally symmetry and can be defined by a function of a single variable, the distance r from the origin,

$$b_{m,a,\alpha}(r)=\begin{cases}\dfrac{\left[\sqrt{1-\left(\frac{r}{a}\right)^2}\right]^m}{I_m(\alpha)} I_m\left[\alpha\sqrt{1-\left(\frac{r}{a}\right)^2}\right] & if \quad 0\le r\le a;\\ 0 & otherwise\end{cases} \tag{2}$$

I_m : modified Bessel function of order m;
a : radius of support of the blob;
α : a parameter controlling the shape of the blob.

Figure 1 shows the profiles of three types of blobs by selecting different parameters value for a and α.

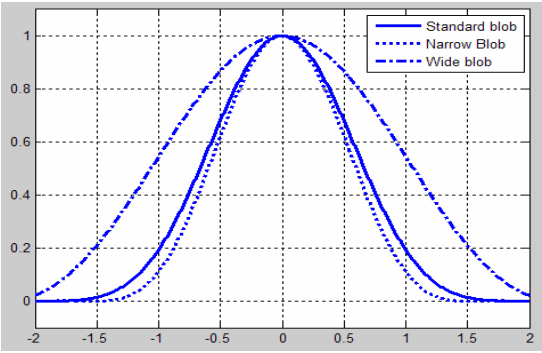

Figure 1 : Profiles of a standard blob, a narrow blob and a wide blob

B. Discretisation of Imaging Model in Super-Resolution

In [18], it is assumed that a set of low-resolution images were produced by a single high-resolution image, the generative imaging model for one low-resolution image is

$$g_i(x,y)=s\downarrow[h(u,v)*f(T_i(x,y))]+\eta_i(x,y) \tag{3}$$

where

g_i is the i^{th} observed low-resolution image;
f is the ground truth, high-resolution image;
T_i is the geometric transformation of i^{th} image;
h is the point-spread function (PSF);
s↓ is the down-sampling operator by a factor s;
η_i is the observation noise.

From the imaging model, we know that each low-resolution pixel is therefore a weighted sum of super-resolution pixels, the weights being determined by the registration parameters, the point-spread function and spatial integration. In order to explain the model in a simpler way, we drop other explicit photometric parameters. The model can be expressed in matrix form as an over-determined linear system :

$$\mathbf{g}=\mathbf{M}f+\boldsymbol{\eta} \quad \text{or} \quad \begin{bmatrix}g_1\\g_2\\\vdots\\g_i\\\vdots\\g_n\end{bmatrix}=\begin{bmatrix}M_1\\M_2\\\vdots\\M_i\\\vdots\\M_n\end{bmatrix}f+\begin{bmatrix}\eta_1\\\eta_2\\\vdots\\\eta_i\\\vdots\\\eta_n\end{bmatrix} \tag{4}$$

Capel derived a maximum likelihood estimate, f_{mle} for the super-resolution image f, given the measured set of low-resolution images, $\mathbf{g}$ and imaging matrix, $\mathbf{M}$. Assuming the image noise to be Gaussian with zero mean, variance, σ^2; the total probability of an observed image, $g_i(x,y)$ given an estimate of the super-resolution image, $\hat{f}(x,y)$ is

$$\Pr(g\mid\hat{f})=\prod_{\forall x,y}\frac{1}{\sigma\sqrt{2\pi}}\exp\left(-\frac{(\hat{g}_i(x,y)-g_i(x,y))^2}{2\sigma^2}\right) \tag{5}$$

where a simulated low-resolution image is $\hat{g}_i=M_i\hat{f}$

The corresponding log-likelihood function is

$$L(g_i)=-\sum_{\forall x,y}(\hat{g}_i(x,y)-g_i(x,y))^2=-\|\hat{g}_i-g_i\|=-\|M_i\hat{f}-g_i\| \tag{6}$$

The log-likelihood over all images is

$$\sum_{\forall n}L(g_i)=-\sum_{\forall x,y}\|M_i\hat{f}-g_i\|^2=-\|\mathbf{M}f-\mathbf{g}\|^2 \tag{7}$$

The estimate which maximizes the log-likelihood over all images is

$$f_{mle}=\arg\min_f\|\mathbf{M}f-\mathbf{g}\|^2 \tag{8}$$

The optimum $\hat{f}_{mle}$ is given by

$$\hat{f}_{mle}=(\mathbf{M}^T\mathbf{M})^{-1}\mathbf{M}^T\mathbf{g}=\mathbf{M}^+\mathbf{g} \tag{9}$$

where $\mathbf{M}^+$ is the Moore-Penrose pseudo-inverse of $\mathbf{M}$.

III. Incorporating Blobs into Super-Resolution Framework

In this section, we propose a novel approach by incorporating the basis functions, blobs, into the super-resolution reconstruction framework. Before we introduce the approach, let us first look into how Capel computed the above matrix, $\mathbf{M}$.

In order to compute the $\mathbf{M}$ matrix, the intensity value of each low-resolution pixel is given by an area integral over the geometrically warping of the original (super-resolution) image, weighted by a PSF,

$$\int_0^1\int_0^1 f_{xy}h_{psf}\,dxdy \tag{10}$$

Each row in a matrix, $\mathbf{M}_i$ is therefore a discretisation of the integral of the surface $f\times h_{psf}$ for a single pixel in the

corresponding low-resolution image, $g_i(x,y)$. The mapping between a low-resolution image and the super-resolution image is accomplished by using homographic (affine) transformation of the Gaussian PSF. Each Gaussian PSF is mapped onto the homography under local affine transformation using approximation.

During the warping of the super-resolution pixels, we assume that the super-resolution image is actually made up of a set of coefficients and the known basis functions; in this case we choose blobs. Similar to the previous approach, the super-resolution image (represented using blob elements in our novel approach) undergoes geometrical warping, weighted by a PSF.

The new algorithm :

- Compute the local warping (affine transformation) about the centre of low-resolution pixel, (x_0, y_0) onto the super-resolution frame;
- Transform the parameters of the Gaussian PSF centred at (x_0, y_0) using the same affine transformation and determine a truncated ellipse of the Gaussian PSF, say using 3 standard deviation;
- Scan-convert the ellipse to obtain the set of super-resolution pixels using blobs as its basis functions, centred at (x_0, y_0);
- Evaluate the coefficients for the warped super-resolution frame within the truncated Gaussian PSF ellipse, weighted using blob basis functions;
- Normalise the row of the imaging matrix such that its sum is equal to 1.

IV. Experiments for Justification and Results

In order for us to justify that our new super-resolution algorithm based on blobs can give better reconstruction results, we have selected two different synthetic images for experimental justification. In both sets of experiments, we have chosen some suitable parameters for the super-resolution imaging model, with increasing noise. Both the point-spread function and the image noise are assumed to be Gaussian. We have used 'standard' blob parameters for our blob-based super-resolution reconstructions.

We have chosen a 32x32 pixels 'text' image as our original (super-resolution) image in our first set of experiments since it has high contrast with fine detail. We used a 32x32 pixels synthetic phantom with four different grey-levels which are coarsely quantized in our second set of experiments. *Figure 2* shows the two synthetic images used in our experiments.

The quality of super-resolution reconstruction obtained using the maximum-likelihood estimator (MLE) depends on several factors :

- number of low-resolution images available
- up-sampling ratio
- accuracy of the geometric registration
- noise on the observed images
- size and accuracy of the PSF

Figure 2 : Synthetic images used for super-resolution reconstruction

We know that the MLE is extremely sensitive to noise sources, including image noise and model noise, especially when there are inaccuracies in the design of the PSF and the registration parameters.

From our previous experiences as well as the parameters selected in [18], we have chosen some suitable values for the registration parameters, σ_H, the Gaussian PSF, σ_{psf} and the down-sampling ratio, s↓ in our generative imaging model as in *Equation (3)* when using the model to generate low-resolution images from the synthetic images.

Experiment Set I

Figure 3 shows a series of low-resolution images used in this set of experiments with increasing Gaussian image noise added while other parameters remain fixed.

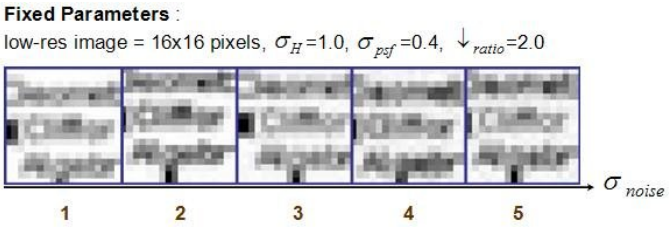

Figure 3 : Low-resolution images used for super-resolution reconstruction

Figure 4 shows the results of a set of 25 experiments obtained, each with the selected parameters, different number of low-resolution images versus various image noise added.

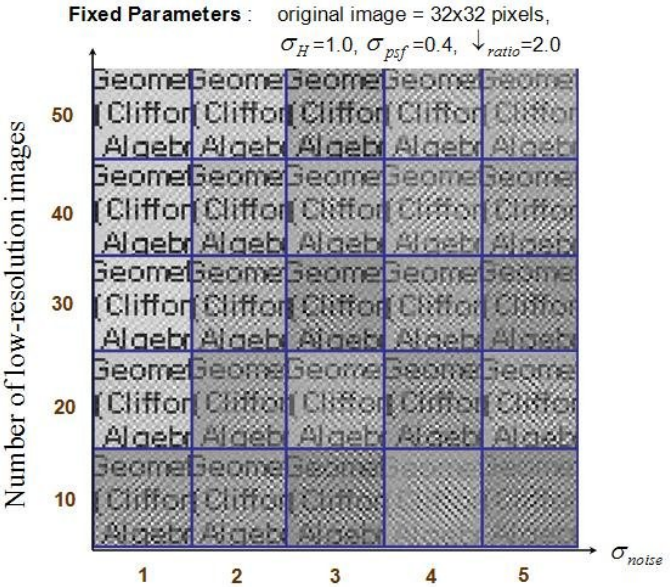

Figure 4 : Reconstructed super-resolution images using the MLE

Each column in the figure shows the recovery of the super-resolution reconstructions by the MLE in *Equation (9)* using different number of low-resolution images generated from the imaging model. This set of experiments is only repeating Capel's approach of using pixels as the basis functions for the super-resolution reconstruction.

Figure 5 shows a series of low-resolution images similar to the above set of experiments except at this time we used blobs as the basis functions for the super-resolution reconstruction.

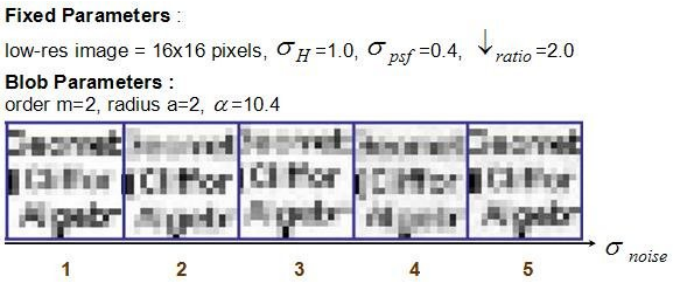

Figure 5 : Low-resolution images used for super-resolution reconstruction with blobs as its basis functions

Figure 6 shows the results of a set of 25 experiments obtained, using blobs as the basis functions for the image reconstruction, each with the selected parameters, different number of low-resolution images versus various image noise added.

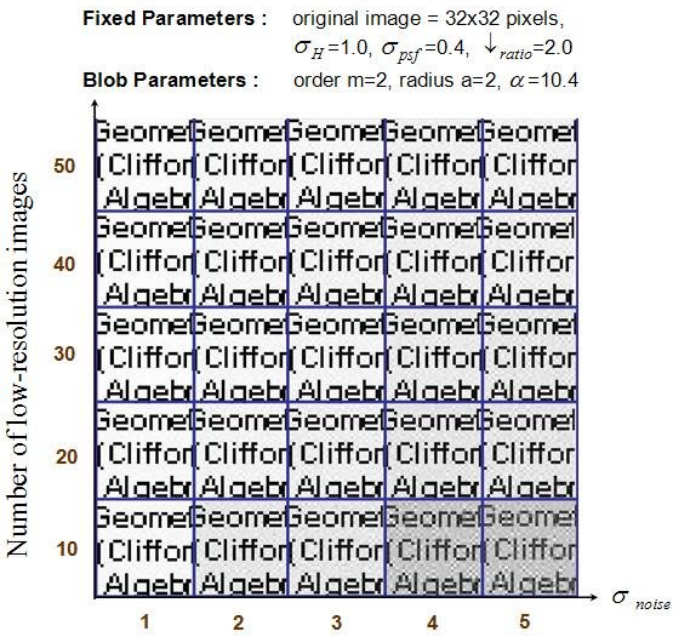

Figure 6 : Reconstructed super-resolution images using the MLE with blobs as its basis functions

Each column in *Figure 6* also shows the recovery of the super-resolution reconstructions by the MLE in *Equation (9)* using different number of low-resolution images generated from the imaging model.

From the results obtained, only by qualitative observation, it is very encouraging to say that the super-resolution reconstruction algorithm using blobs as the basis functions can recover a set of much better super-resolution images. We shall come to quantitative evaluations of the two set of results in the next section.

Experiment Set II

Similar to *Experiment Set I*, *Figure 7* shows a series of low-resolution images used in this set of experiments with increasing Gaussian image noise added while other parameters remain fixed.

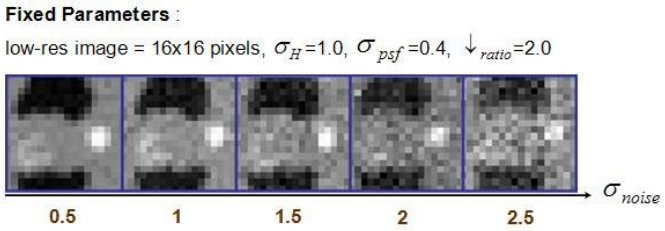

Figure 7 : Low-resolution images used for super-resolution reconstruction

Figure 8 shows the results of a set of 25 experiments obtained, each with the selected parameters, different number of low-resolution images versus various image noises added, except at this time reconstruction of the synthetic image is more sensitive to noise. Each column in the figure shows the recovery of the super-resolution reconstructions by the MLE in *Equation (9)* using different number of low-resolution images generated from the imaging model. This set of experiments only repeats Capel's approach of using pixels as the basis functions for the super-resolution reconstruction.

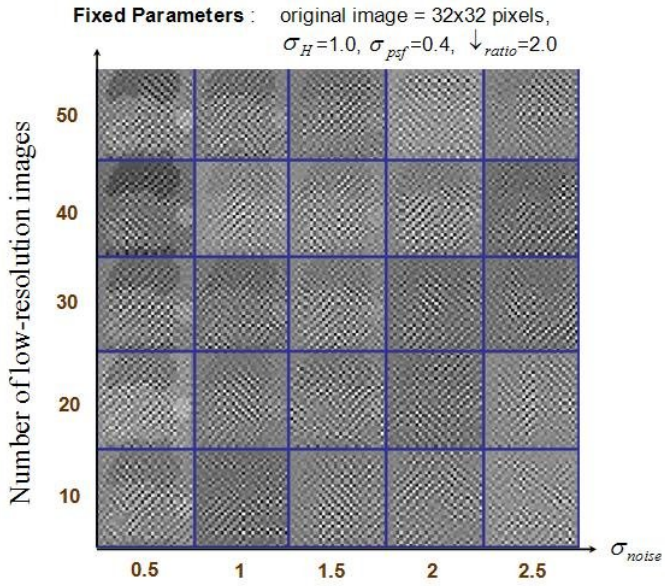

Figure 8 : Reconstructed super-resolution images using the MLE

Figure 9 shows a series of low-resolution images similar to the above set of experiments except at this time we used blobs as the basis functions for the super-resolution reconstruction.

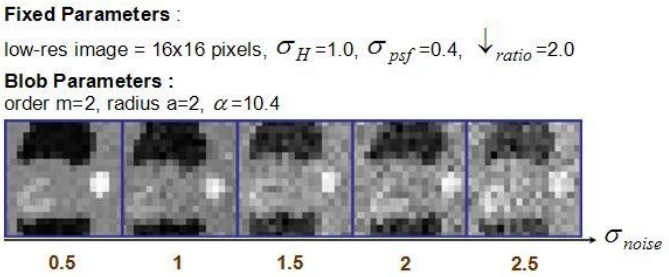

Figure 9 : Low-resolution images used for super-resolution reconstruction with blobs as its basis functions

Figure 10 shows the results of a set of 25 experiments obtained, using blobs as the basis functions for image reconstruction, each with the selected parameters, different number of low-resolution images versus various image noise added.

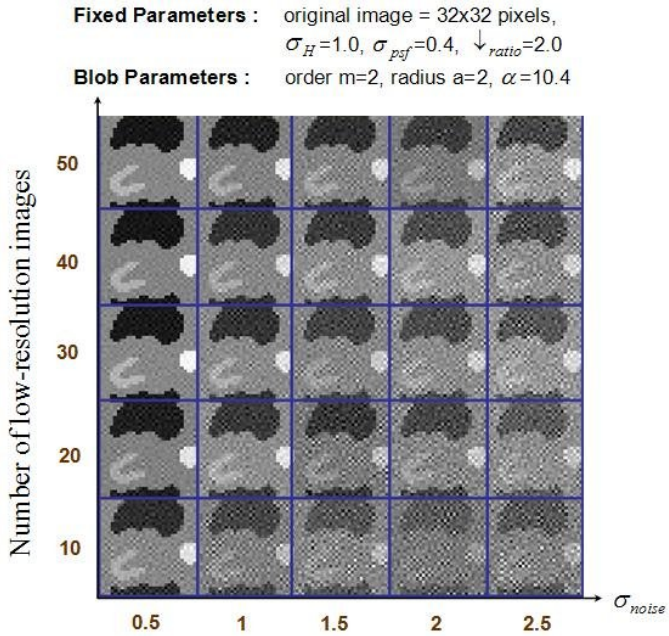

Figure 10 : Reconstructed super-resolution images using the MLE with blobs as its basis functions

Each column in *Figure 10* also shows the recovery of the super-resolution reconstructions by the MLE in *Equation (9)* using different number of low-resolution images generated from the imaging model.

Again, from the results obtained, we can see that this synthetic image used for super-reconstruction is more sensitive to noise. Without using blobs as the reconstructed image basis functions, we can hardly identify the properties of the original image.

V. Discussion

In order for us to make quantitative evaluation of the experimental results, we have calculated the root-mean-square errors (RMSE) for each set of the results obtained.

Figure 11 and *Figure 12* respectively show the RMSE per pixel between the original synthetic 'text' image used in the *Experiment Set I* comparing the reconstructed super-resolution images without and with using blobs as its basis functions, using different numbers of low-resolution images generated with increasing Gaussian image noise while other imaging model parameter remained fixed.

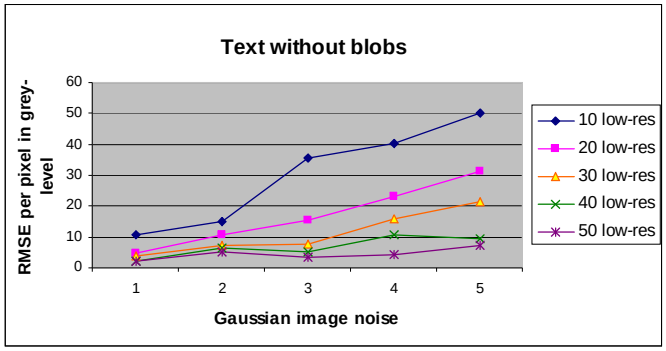

Figure 11 : RMSE per pixel for different number of low-res images used in reconstruction against Gaussian image noise for 'text' image without blobs

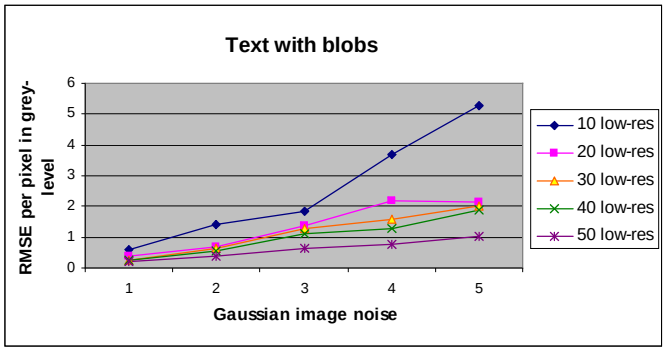

Figure 12 : RMSE per pixel for different number of low-res images used in reconstruction against Gaussian image noise for 'text' image with blobs

From the above figures, we can see that using blobs as the basis functions in the super-resolution reconstructions, we obtained almost 10 times more accurate results compared with those reconstructed super-resolution images without using blobs as basis functions.

Figure 13 and *Figure 14* respectively show the RMSE per pixel between the original synthetic phantom image used in the *Experiment Set II* comparing the reconstructed super-resolution images without and with using blobs as its basis functions, using different numbers of low-resolution images generated with increasing Gaussian image noise while other imaging model parameter remained fixed.

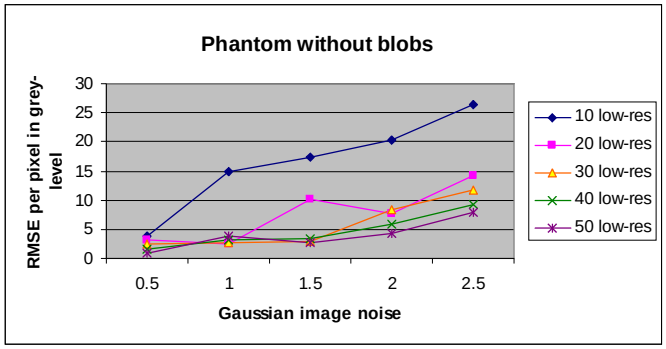

Figure 13 : RMSE per pixel for different number of low-res images used in reconstruction against Gaussian image noise for phantom image without blobs

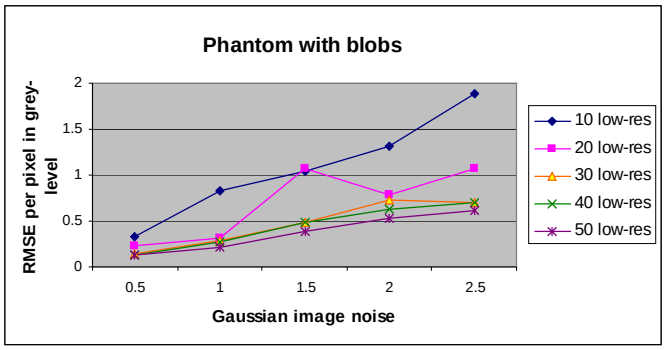

Figure 14 : RMSE per pixel for different number of low-res images used in reconstruction against Gaussian image noise for phantom image with blobs

From the figures, we can also see that using blobs as the basis functions in the super-resolution reconstructions, we obtained approximately 10 times more accurate results compared with those reconstructed super-resolution images without using blobs as its basis functions. From *Experiment Set I* and *II* the synthetic phantom image is more sensitive to image noise than the 'text' image because it contains more grey-level variations.

VI. Conclusion

Many different approaches have been suggested to further improve the quality of super-resolution reconstructions, such as using splines and interpolations. Higher-order interpolation methods, particularly smoothing splines, can perform better, but they tend to blur the image. In contrast, blobs act as low-pass filters suppressing high-frequencies noise but not blurring the image.

In this paper, we have proposed a novel approach by incorporating Kaiser-Bessel window functions (blobs) as the image basis functions in the super-resolution reconstruction framework. We obtained excellent reconstruction results that guarantee saving computational time and giving a much better quality of recovered image compared with reconstruction results of other super-resolution framework using normal pixels as their basis functions. Obviously, our framework can easily be extended to 3-D super-resolution reconstructions where we replace voxels with 3-D blobs as the basis functions.

Although we have chosen a slightly high registration error relative to the image size in our experiments in order for us to emphasize that using blobs as the basis functions can actually recovered much better quality reconstructions, one can certainly use lower registration error according to raw data obtained from commercial cameras or medical imaging scanners, which depends on the ability of those equipments. Using lower registration error relative to other parameters, we should obtain a linear relationship between the RMSE and the image noise (reconstruction error versus the observation noise).

Since we chose to use synthetic images in our experiments, where low-resolution images were generated from the imaging model, one can actually uses raw acquired low-resolution data without assuming that blobs were used as their basis functions, one can still obtain similar improvement on the super-resolution reconstruction.

We believe that this is the first paper where this novel approach of incorporating blobs into super-resolution reconstruction framework has been presented. We only used standard blobs to deliver the results. However, further improvement can be seen if we were to use optimized blobs that are best suited with other reconstruction parameters. Normally, selecting optimized blobs for super-resolution reconstructions depends on a few criteria such as down-sampling ratio, registration error and image noise of the raw data.

References

[1] R. M. Lewitt. *Multidimensional digital image representation using generalized Kaiser-Bessel window functions*. J. Optical Soc. Amer. A., 7 : 1834-1846, 1990.

[2] R. M. Lewitt. *Alternatives to voxels for image representation in iterative reconstruction algorithms*. Phys. Med. Biol., 37(3) : 705-716, 1992.

[3] S. Matej and R. M. Lewitt. *Efficient 3D grids for image reconstruction using spherically symmetric volume elements.* IEEE Trans. Nucl. Sci., 42(4) : 1361-1370, 1995.

[4] S. Matej and R. M. Lewitt. *Practical considerations for 3D image reconstruction using spherically symmetric volume elements.* IEEE Trans. Med. Imag., 15 : 68-78, 1996.

[5] H. Ur and D. Gross. *Improved resolution from subpixel shifted pictures*. Graphical Models and Image Processing, 54(2) : 181-186. 1992.

[6] R. Tsai and T. Huang. *Multi-frame image restoration and registration*. Advances in Computer Vision and Image Processing, 1 : 317-339, 1984.

[7] M. Elad and A. Feuer. *Super-resolution reconstruction of image sequences*. IEEE Trans. Pattern Analysis and Machine Intelligence, 21(9) : 817-834, 1999.

[8] P. E. Eren, M. I. Sezan and A. M. Tekalp. *Robust, object based high-resolution image reconstruction from low-resolution video*. Proc. IEEE Int. Conf. Image Processing, pp.176, 1996.

[9] N. Nguyen, P. Milanfar and G. H. Golub. *A computationally efficient image super-resolution algorithm*. IEEE Trans. Image Processing, 10(8) : 1187-1193, Aug. 2001.

[10] M. Elad. *Super-resolution reconstruction of images*. PhD thesis, Technion, Isreal. 1996.

[11] M. Irani and S. Peleg. *Motion analysis for image enhancement : resolution, occlusion and transparency*. J. Visual Communication and Image Representation, 4:324-335, 1993.

[12] D. Capel and A. Zisserman. *Automated mosaicing with super-resolution Zoom*. Proc. IEEE Conf. Computer Vision and Pattern Recognition, Santa Barbara, pp. 885-891, 1998.

[13] M. Irani and S. Peleg. *Improving resolution by image registration*. Graphical Models and Image Processing, 53:231-239. 1991.

[14] M. V. Joshi and S. Chaudhuri. *Super-resolution imaging : use of zoom as a cue.* Proc. Indian Conf. Vision, Graphics and Image Processing, Ahmedabad, India, pp. 439-444, Dec. 2002.

[15] D. Rajan and S. Chaudhuri. *A generalized interpolation scheme for image scaling and super-resolution.* Proc. Erlangen Workshop on Vision, Modelling and Visualisation, University of Nuremberg, Germany, pp. 301-308, Nov. 1999.

[16] D. Rajan and S. Chaudhuri. *Generalised interpolation and its applications in super-resolution imaging.* Image and Vision Computing, Vol. 19, pp. 957-969, Nov. 2001.

[17] S. Chaudhuri. *Super-resolution imaging*. Kluwer Int. Series in Engineering and Computer Science ; SECS 632, 2002.

[18] D. P. Capel. *Image Mosaicing and super-resolution*. PhD thesis, University of Oxford, Trinity Term, 2001.